Investigation of Different Rules Size FLSC Performance Applied to Induction Motor Drive

M. H. N. Talib, Z. Ibrahim, Z. Rasin, J. Mat Lazi, M. Azri
Faculty of Electrical Engineering, Universiti Teknikal Malaysia Melaka,
Hang Tuah Jaya, 76100 Durian Tunggal, Melaka
hairulnizam@utem.edu.my

***Abstract*—Fuzzy Logic Controller (FLC) has been widely used in speed controller due to its superior performance results. It is suitable when the system is difficult to model mathematically due to its nonlinearity and complexity. There are three common number of rules design which are commonly used in FLSC known as 49, 25 and 9 rules. However, the majority of the previous research report mainly focused on the dedicated rules size design either 49, 25 or 9 rules for the optimum performance. There is lack of performance comparison between 49, 25 and 9 rules size. Thus, it is difficult to understand how the rules size affects the motor performance. This research tries to fill up the gap by comparing the controller performance using the same platform. The fuzzy logic speed controllers (FLSC) with a different type of rules base are applied to the induction motor drive system. The FLSC with 49, 25 and 9 rules are investigated through MATLAB/SIMULINK and performance comparisons are made covering a wide speed range operations and load disturbance. The simulation results are evaluated based on the rise time (T_r), overshoot (OS), settling time (T_s), Integral Absolute Error (IAE) and Integral Time Absolute Error (ITAE) for transient and steady state condition. It is shows that the smaller size of rules does not necessarily degrade the performance.**

***Index Terms*—Induction Motor; FLC; Speed Drive; Fuzzy Rules.**

I. Introduction

The induction motor is one of the important workhorse for industrial applications due to the working capability, lower price and simple structure. The invention of vector control and direct torque control method increases the popularity of this motor to replace the DC motor drive, especially for variable speed drive application. The proportional integral controller is integrated with this modern drive system to control the system performance. This conventional controller, however, depends too much on the motor parameters accuracy and load disturbances [1-3]. Any change in these parameters may degrade the overall performance.

For the last four decades, the fuzzy logic controller has become as one of the choices available for a speed controller. This is due to the merit of its easy implementation, parameter independence and capability of handling a nonlinear system [4]. Therefore, the FLC has demonstrated a better performance capability and becomes one the favorite alternative for the high-performance speed drive application [1, 2]. Furthermore, the implementation of FLC is also able to improve the robustness of the system performance [5].

Progressively, many researches have been focused on the design of FLC [6, 7]. Majority of the FLC studied for the drive application are focused on the superiority of the FLC performance over the conventional controller. The discussion mainly focused on the FLC design and tuning approach to achieve the optimum performance. The discussion, however, is limited to the proposed FLC approach. The early design of FLC used the 49 rules with triangular and trapezoid membership function (MF) shape. Due to the complexity of the algorithm, the numbers of rules are reduced to 25 and 9. Thus, the majority of the researches can be classified based on the number of rules used either 49, 25 or 9[1, 3, 8]. However, there is still lack of performance comparison analysis between these fuzzy rules based controller under one platform. In general, the larger numbers of rules significantly affect the computation burden and memory space requirement.

The earliest investigation on the effect of the fuzzy rule was discussed by I. Eminoglu and I. H. Altas [9], applied to the PM DC motor. The studies investigate the number of rules effect on the average output of the controller. The decision rules are tuned to control the DC chopper and significantly different to the common speed control decision rules table. In addition, the distributions of the triangular membership function are in asymmetrical form. The outer MFs subsets are removed in order to reduce the number of rules from 7 to 5 and finally 3. The final 3 MF subsets are maintained for all fuzzy set. Another study conducted in 2000 by Betin analyzed the effect of a number of rules applied to the stepper motor drive [10]. Four numbers of rules discussed with an addition of 81 rules set. The performance comparison, however, is limited to the rated speed operation and used to choose the most suitable fuzzy set number. Based on the finding, the use of 81 rules does not improve the accuracy and increases the computation burden. As a conclusion, 49 fuzzy rules are the most suitable.

Investigation of different rules based FL speed controller on the induction motor drive was done by B. Kumar et al [11]. Performance comparisons are made between 49, 25 and 9 rules, showing an excellent performance for the 49 rules but it results in higher computational burden. The analysis is also limited to the transient operation for the forward-bias operation. A wider selection of speed ranges covers for forward and reverse at low, medium and high-speed operations are important for the investigation. Different rules based size analysis is related to the difference in the fuzzy set distribution coverage. In addition, symmetrical and equally distributed of triangular and trapezoid MF shapes are used with 50% overlapping between the adjacent MFs.

This paper discusses the FLSC with different rules based size applied on the dynamic model of induction motor drive system. The analysis is detailed, covering from high, medium and low-speed operation for load and unloaded condition. The Integral Absolute Error (IAE) and Integral Time

Absolute Error (ITAE) performance measures are used to evaluate the overall dynamic performance.

II. INDUCTION MOTOR DRIVE SYSTEM

Figure 1 shows the overall field oriented control (FOC) of an induction motor drive schematic diagram. The diagram consists of the induction motor model, voltage source inverter with hysteresis current controller, indirect FOC method and two to three phase transformation.

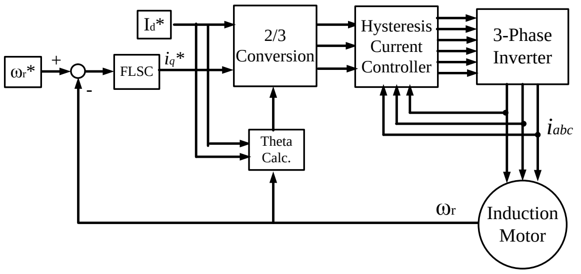

Figure 1: FOC block diagram fed by hysteresis current controller

The mathematical equation of induction motor is modeled in the synchronous rotating frame as discussed in [12]. Based on the indirect FOC principle, the rotor flux angle, θ_e for coordinate transformation is generated from the integration of rotor speed, ω_r and slip frequency, ω_{sl} as shown in Equation (1).

$$\theta_e = \int (\omega_r + \omega_{sl})\, dt \tag{1}$$

The slip frequency is calculated by using Equation (2) and included in theta calculation block.

$$\omega_{sl} = \frac{L_m}{\tau_r}\frac{i_{sq}}{\varphi_r} \tag{2}$$

For the variable speed drive application, ω_r^* is chosen as a reference signal to control the speed of the induction motor. The actual speed of the motor (ω_r) is compared with the reference speed (ω_r^*). The instantaneous state of the speed error is regulated by the fuzzy logic speed controller (FLSC) to produce the torque, i_q^* current reference. The torque, i_q^* and flux, i_d^* currents reference are transformed from two to three phase current reference. The stator actual currents and the above three phase reference currents are synthesized in the hysteresis current controller to generate the switching signals for the inverter. The current error bandwidth is set at ±0.2A to control the output of the inverter voltage. The similar schematic diagram is modeled and simulated using the MATLAB/SIMULINK software.

III. FLSC DESIGN

This study is focused on the different number of rules based applied for the FLSC. Figure 2 shows the FLC block diagram.

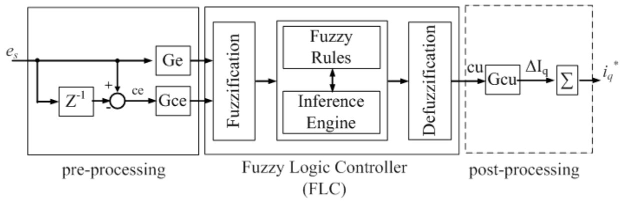

Figure 2: Fuzzy logic controller block diagram

The speed error, e and the change of speed error, Δe are two inputs variable. During preprocessing, the inputs variables are normalized by input gain scaling factor, G_e and G_{ce} respectively. The normalized inputs variable signals are fed through the fuzzification process by the input membership function. The numerical inputs variables are transformed into the linguistic variable. The membership functions are chosen to cover the entire universe of discourse. Then the linguistic signals are synthesized based on the fuzzy rules, reasoning mechanism and database using the Mamdani fuzzy rules base system. The fuzzy rules map the input and output linguistic variables. In this research, the 49, 25 and 9 rules based are chosen for the analysis. Finally, the defuzzified process changes the linguistic variable into crisp values to provide a crisp value such as change-of-control. The rules and MFs are designed using the FIS editor in Matlab software. The program generated is integrated with the model of the induction motor in the Simulink environment for the simulation investigation.

A. Membership Function

Forming the MFs is an important task to represents the system responses. Using the triangular and trapezoidal shapes provides the best performance with a lower computation burden [13]. The MFs are arranged to have a symmetrical distribution with 50% overlap between the adjacent MFs to prevent from minor changes in the inputs. Figure 3 shows the error (e), change of error (ce) and change of output control (cu) membership function for 49, 25 and 9 rules based respectively.

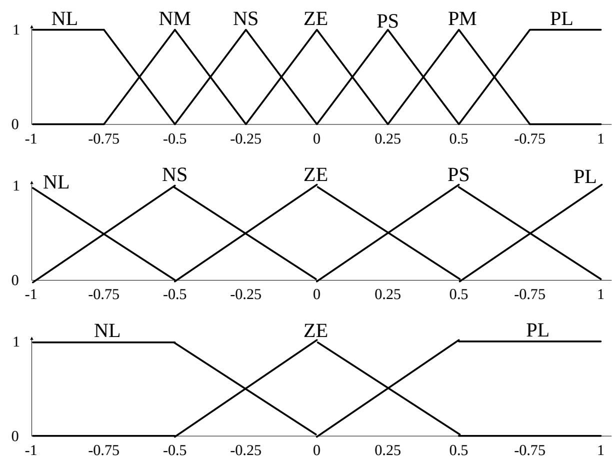

Figure 3: Membership functions for e, ce and cu. (a) 49 rules; (b) 25 rules; (c) 9 rules.

B. Scaling Factor Determination

The initial scaling factor is based on the maximum magnitude of the speed when the motor is running at a rated speed error during forward operation. The error gain SF can be determined by the following equation [14]:

$$G_e = \frac{1}{|2\omega_{emax}|} \tag{3}$$

Meanwhile, the SF for change of error is determined based on the change of error demand. Thus, the G_{ce} can be determined by Equation (4) [14]:

$$G_{ce} = \frac{1}{\Delta\omega_{max}} \tag{4}$$

Finally, the G_{ce} is tuned manually at rated speed operation to achieve a zero overshoot with faster response. Through several simulations test, the final value for the G_e, G_{ce} and G_{cu} are 3.34m, 1.15m and 1 respectively.

C. Forming rule decision table

The rules base that decides the output of the inference system consists of 49, 25 and 9 rules based on the inputs and output of the MFs set. The rules are developed based on the characteristic of the step response and phase plane trajectory method is used to map the inputs and output rules [15, 16]. Figure 4 shows the rules matrix for the 49, 25 and 9 rules.

e(k) / ce(k)	**NL**	**NM**	**NS**	**ZE**	**PS**	**PM**	**PL**
NL	NL	NL	NL	NL	NM	NS	ZE
NM	NL	NL	NL	NM	NS	ZE	PS
NS	NL	NL	NM	NS	ZE	PS	PM
ZE	NL	NM	NS	ZE	PS	PM	PL
PS	NM	NS	ZE	PS	PM	PL	PL
PM	NS	ZE	PS	PM	PL	PL	PL
PL	ZE	PS	PM	PL	PL	PL	PL

(a) 49 rules, (7x7)

e(k) / ce(k)	**NL**	**NS**	**ZE**	**PS**	**PL**
NL	NL	NL	NL	NS	ZE
NS	NL	NS	NS	ZE	PS
ZE	NL	NS	ZE	PS	PL
PS	NS	ZE	PS	PS	PL
PL	ZE	PS	PL	PL	PL

(b) 25 rules, (5x5)

e(k) / ce(k)	**NL**	**ZE**	**PL**
NL	NL	NL	ZE
ZE	NL	ZE	PL
PL	ZE	PL	PL

(c) 9 rules, (3x3)

Figure 4: Rules distibution for; (a) 49 rules; (b) 25 rules; (c) 9 rules.

IV. SIMULATION AND DISCUSSION

For the performance evaluation, the proposed speed controller is applied to the 1.5 kW induction motor drive system fed by SVPWM using Simulink/Matlab software as shown in Figure 1. The parameters of the motor are shown in Appendix A. The voltage supply is set at rated voltage 537 Vdc with 8 kHz switching frequency for the inverter. All the inputs and output gain scaling factors and membership function distribution is kept constant for all sets of rules as determined in Section 3. The speed performances of the induction motor drive are investigated with different fuzzy rules set based on 49, 25 and 9 rules. The performance comparison is made under different operation condition such as step input for low, medium and high-speed reference and load disturbance.

A. Rated speed operation

For this test, the speed of the motor is set to operate at 1400rpm from stand still at 0.5s. The rated load is applied between 1.5s to 2.5s. Finally, the speed demand is changed for reverse operation at 3s. Figure 5 shows the speed and torque current response of the rules. In overall observation, the performances of the motor are similar for R49, R25 and R9. There is a good correlation between speed and torque current behavior. Further verification, however, shows a small performance discrepancy during transient response at the start up and during the load disturbance as shown in the close up view. The R49 produce a faster response to reach the speed demand followed by R25 and R09. Meanwhile, R49 recorded the smallest speed drop, followed by R09 and R25.

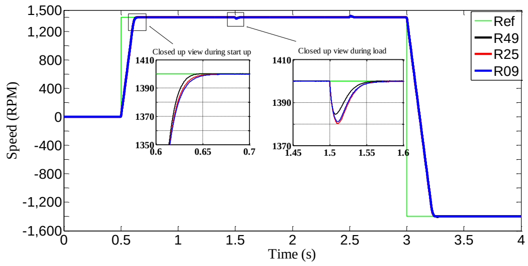

(a) Speed performance

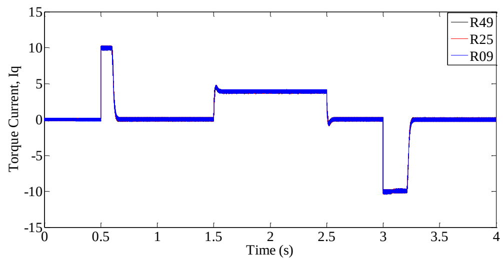

(b) Torque current performance

Figure 5: Speed and torque current response obtained for 49, 25 and 9 rules at 1400 rpm.

Details performance of the rise time, T_r and load disturbance are shown in Table 1 and Table 2. The rise time is measured between 0 to 90% of the speed demand. Based on the rise time performance, R09 produces the fastest time compared to others during forward speed operation. Meanwhile, for reverse speed operation, all rules produce a similar rise time when the speed is changed from 1400 rpm to -1400 rpm.

Table 1
Forward and Reverse Speed Operation at Rated Speed

Rules	Forward, T_r	Reverse, T_r
49	0.1035s	0.2040s
25	0.1035s	0.2040s
9	0.1031s	0.2040s

Table 2 tabulates the speed drop and recovery time comparison. The smallest speed drop is recorded for R49 with 15 rpm. Meanwhile, the R25 and R09 records a speed drop of 20 rpm and 19 rpm respectively. The R49 rules lead the recovery time, followed by R25 and R09 with 56.9% and 69.2% longer time respectively.

Table 2
Load Disturbance at Rated Speed Operation

Rules	Speed drop, SD	Recovery Time, RT
49	15 rpm	0.065s
25	20 rpm	0.102s
9	19 rpm	0.110s

B. Medium and Low-speed operation

Figure 6 shows the performance comparison at 100 rpm, 500 rpm and 1000 rpm to represent the low and medium speed operation. Figure 6(a) shows the overall speed command. The similar testing procedure is applied for this test as set for the rated speed operation. Meanwhile, Figure 6(b) and 6(c) show the close-up view during start up and loaded condition at different speed demand. Similar performance behavior to the rated speed operation is recorded as well.

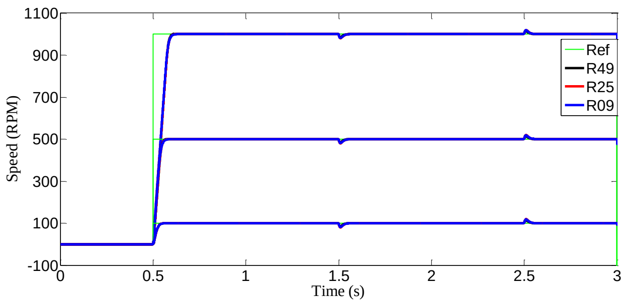

(a) Overall speed response

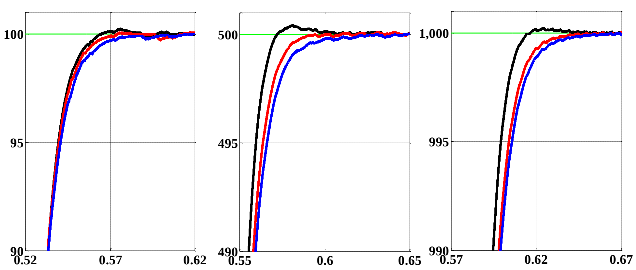

(b) Close up view during start up

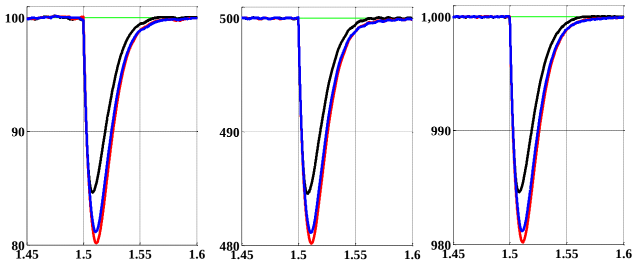

(c) Close up view during load disturbance

Figure 6: Speed response at 1000, 500 and 100 rpm speed demand for 49, 25 and 9 rules.

Table 3 tabulates the rise time (T_r), speed drop (SD), and recovery time (T_{rt}) at 1000 rpm, 500 rpm and 100 rpm speed demand with rated load disturbance. Based on the transient response, R09 leads the rise time response. Interestingly, the faster rise time performance does not guarantee the response to have a better settling time towards the reference speed. Meanwhile, R49 rules give superior performance when external load disturbance is applied compared to the others. The R09 shows a better performance compared to the R25 in term of the speed drop, but not for the recovery time. The higher numbers of rules improve the settling time.

Table 3
Transient Response at 1000 rpm, 500 rpm and 100 rpm Demand

Speed (rpm)	Rules	T_r	SD (rpm)	T_{rt} (s)
	49	0.0756	15.40	0.064
1000	25	0.0759	19.80	0.120
	9	0.0751	18.80	0.124
	49	0.0431	15.40	0.062
500	25	0.0435	19.80	0.114
	9	0.0431	18.90	0.114
	49	0.0332	15.37	0.064
100	25	0.0331	19.87	0.107
	9	0.0335	18.70	0.123

C. ITEA and IAE performance measures

IAE and ITAE performance indicators have an advantage in numerically evaluating the quality of the dynamic performance based on integral expression of the control error. The IAE index reflexes the cumulative error with respect to the reference. Meanwhile, the ITAE represents the integral of the absolute value multiplied by time. The error is referred to the speed deviation between the reference and the actual response. This performance measurement covers for transient and steady state operations during load and unloaded condition. Further simulation analyses based on this performance measurement are conducted as the test condition discussed in Section 4.A. The analysis results of the ITAE and IAE performance index for wide speed ranges operations are shown in Table 4.

Table 4
ITAE and IAE Performance Index for Wide Range Operation

Rules	Index	1400 rpm	1000 rpm	500 rpm	100 rpm
R49	ITAE	107.3	54.68	14.09	1.425
	IAE	41.89	21.64	5.728	0.6577
R25	ITAE	107.4	54.95	14.23	1.465
	IAE	42.05	21.75	5.781	0.6789
R09	ITAE	107.4	54.84	14.15	1.437
	IAE	41.97	21.64	5.729	0.6679

Based on the comparison, R49 shows superiority dynamic performance compared to others with smaller ITAE and IAE index followed by R09 and R25. Even though the R25 has a bigger number of rules, this does not guarantee a better performance. The speed performances are also dependent on the distribution of the MFs.

V. CONCLUSION

This paper presents the performance comparison between different rules based FLSC applied to the induction motor drive. Three commonly used rules based size have been simulated in Matlab/Simulink environment. In overall observation, the performances of the motor are very similar for R49, R25 and R9. Details comparison, however, shows 49 rules based FLSC gives superior results compared to the 25 and 9 rules. The 9 rules base, however, shows a faster rise time in low, medium and rated speed range with a very small variation. Meanwhile, 49 rules exhibit a better performance in terms of settling time, speed drop and recovery time as well as ITAE and IAE index. Based on the investigation, the higher number of rules generally improves the steady state error, settling time and load rejection capability. However, the smaller rules size somehow does not necessarily degrade the overall performance of the 25 and 9 rules based FLSC.

APPENDIX A

INDUCTION MOTOR PARAMETERS

$V_S(rated) = 380V$, $f_S(rated) = 50Hz$, $\mathrm{P}(poles) = 4$, $\omega_r(rated) = 1430rpm$, $R_S = 3.45\Omega$, $R_r = 3.6141\Omega$, $L_s = 0.3252\mathrm{H}$, $L_r = 0.3252H$, $L_m = 0.3117H$, $J = 0.02kgm^2$

ACKNOWLEDGMENTS

The authors would like to acknowledge their gratitude to the Universiti Teknikal Malaysia Melaka for providing the resources and support under this short-term grant number PJP/2015/FKE(6B)/S01419.

REFERENCES

[1] Z. Ibrahim and E. Levi, "A Comparative Analysis of Fuzzy Logic and PI Speed Control in High Performance AC Drives using Experimental Approach," *IEEE Transactions on Industry Applications*, Vol. 38, No. 38, pp. 1210-1218, Sep./Oct. 2002.

[2] M. N. Uddin, T. S. Radwan, and M. Azizur Rahman, "Performances of Fuzzy Logic Based Indirect Vector Control for Induction Motor Drive," *IEEE Transactions on Industry Applications*, Vol. 38, No. 38, pp. 1219-1225, Sep./Oct. 2002.

[3] S. Hameed, B. Das, and V. Pant, "Reduced Rule Base Self Tuning Fuzzy PI Controller for TCSC," *International Journal of Electrical Power & Energy Systems*, Vol. 32, No. 32, pp. 1005-1013, Nov. 2010.

[4] B. Bhushan, M. Singh, and P. Prakash, "Performance Analysis of Field Oriented Induction Motor using Fuzzy PI and Fuzzy Logic based Model Reference Adaptive Control," *International Journal of Computer Applications*, Vol. 17, No. 17, pp. 5-12, 2011.

[5] A. Saghafinia, P. Hew Wooi, M. N. Uddin, and K. S. Gaeid, "Adaptive Fuzzy Sliding-Mode Control Into Chattering-Free IM Drive," *IEEE Transactions on Industry Applications*, Vol. 51, No. 51, pp. 692-701, 2015.

[6] F. Gang, "A Survey on Analysis and Design of Model-Based Fuzzy Control Systems," *IEEE Transactions on Fuzzy Systems*, Vol. 14, No. 14, pp. 676-697, 2006.

[7] R. Singh, A. K. Singh, and P. Kumar, "Self-tuned approximated simplest fuzzy logic controller based shunt active power filter," in *International Conference on nergy Economics and Environment (ICEEE)*, 2015, pp. 1-6.

[8] L. Yang, Y. Li, Y. Chen, and Z. Li, "A Novel Fuzzy Logic Controller for Indirect Vector Control Induction Motor Drive," *in 7th World Congress on Intelligent Control and Automation*, 2008, pp. 24-28.

[9] İ. Eminoğlu and İ. H. Altaş, "The Effects of the Number of Rules on the Output of a Fuzzy Logic Controller Employed to a PMDC Motor," *Computers & Electrical Engineering*, Vol. 24, No. 24, pp. 245-261, 1998.

[10] F. Betin, D. Pinchon, and G. A. Capolino, "Fuzzy Logic Applied to Speed Control of a Stepping Motor Drive," *IEEE Transactions on Industrial Electronics*, Vol. 47, No. 47, pp. 610-622, Jun. 2000.

[11] C. Y. Kumar B, Shrivastava V., "Efficacy of Different Rule Based Fuzzy Logic Controllers for Induction Motor Drive " *International Journal of Machine Learning and Computing*, Vol. 2, No. 2, pp. 131-137, 2012.

[12] M. H. N. Talib, Z. Ibrahim, N. A. Rahim, and A. S. A. Hasim, "Comparison Analysis of Indirect FOC Induction Motor Drive using PI, Anti-Windup and Pre Filter Schemes," *International Journal of Power Electronics and Drive Systems (IJPEDS)*, Vol. 4, No. 4, pp. 219-229, 2014.

[13] Z. Jin and B. K. Bose, "Evaluation of Membership Functions for Fuzzy Logic Controlled Induction Motor Drive," in *28th Annual Conference of the Industrial Electronics Society*, 2002, pp. 229-234.

[14] M. H. N. Talib, Z. Ibrahim, N. A. Rahim, and A. S. A. Hasim, "Performance Improvement of Induction Motor Drive Using Simplified FLC Method," in *16th International Power Electronics and Motion Control Conference and Exposition*, Antalya, Turkey, 2014, pp. 843-848.

[15] W. Shun-Chung and L. Yi-Hua, "A Modified PI-Like Fuzzy Logic Controller for Switched Reluctance Motor Drives," *IEEE Transactions on Industrial Electronics*, Vol. 58, No. 58, pp. 1812-1825, 2011.

[16] L. Han-Xiong and H. B. Gatland, "Conventional fuzzy control and its enhancement," *IEEE Transactions on Systems, Man, and Cybernetics, Part B: Cybernetics*, Vol. 26, No. 26, pp. 791-797, Oct. 1996.